Received: 8 September 2021 | Revised: 7 February 2022 | Accepted: 8 February 2022

DOI: 10.1111/jerd.12888

WILEY

RESEARCH ARTICLE

3D-printed resins for provisional dental restorations: Comparison of mechanical and biological properties

Pablo J. Atria DDS, MSci, MPhil[1,2] | Dimorvan Bordin DDS, PhD[3] | Felipe Marti DDS[4] | Vasudev Vivekanand Nayak MSci[5] | Julian Conejo DDS, MSci[6] | Ernesto Benalcázar Jalkh DDS, MSci, PhD[5,7] | Lukasz Witek MSci, PhD[5,8] | Camila S. Sampaio DDS, MSci, PhD[1]

[1]Department of Biomaterials, College of Dentistry, Universidad de los Andes, Santiago, Chile

[2]NYU Grossman School of Medicine, New York University, New York, New York, USA

[3]College of Dentistry, University of Guarulhos, Universus Veritas UNG, Guarulhos, Brazil

[4]Department of Implantology, College of Dentistry, Universidad Mayor, Santiago, Chile

[5]Department of Biomaterials, New York University College of Dentistry, New York, New York, USA

[6]Department of Preventive and Restorative Sciences, University of Pennsylvania School of Dental Medicine, Philadelphia, Pennsylvania, USA

[7]Department of Prosthodontics and Periodontology, University of São Paulo, Bauru School of Dentistry, Bauru, Brazil

[8]Department of Biomedical Engineering, NYU Tandon School of Engineering, New York University, Brooklyn, New York, USA

Correspondence
Pablo J. Atria, Assistant Professor, College of Dentistry, Universidad de los Andes, Monseñor Alvaro del Portillo 12455, Santiago, Chile.
Email: pjatria@miuandes.cl and atria.pablo@gmail.com

Abstract

Objectives: To characterize the mechanical and biological properties of three commercially available resins, which are currently used for provisional restorations and to compare them to an experimental resin intended for definitive fixed dental prostheses.

Materials and methods: Three commercially available resins: Crowntec (CT, Saremco), Temporary C&B (FL, Formlabs), C&B MFH (ND, Nextdent), and the experimental resin: Permanent Bridge (PB, Saremco) were printed and subjected to biaxial flexural strength test, finite element analysis, Weibull analysis, scanning electron microscopy, cell proliferation, immunohistochemistry and cytotoxicity assays. Samples from CT, PB, and ND were provided directly from the manufacturers ensuring ideal workflow. FL was printed using the workflow as recommended by the manufacturer, using a Formlabs 2 printer and their post-processing units Form Wash and Form Cure.

Results: From the tested resins, PB yielded the best overall results in terms of mechanical properties. Cell proliferation and cytotoxicity did not show any significant differences among materials. PB showed higher values for probability of survival predictions (35%) when subjected to 250 MPa loads, whereas the other materials did not reach 10%.

Significance: Despite mechanical differences between the evaluated materials, the outcomes suggest that 3D printed provisional resins may be used in clinical settings, following the manufacturers indications. New materials intended for long-term use, such as the PB resin, yielded higher mechanical properties compared to the other

materials. Alternative printing and post-processing methods have not yet been evaluated and should be avoided until further literature is available.

Clinical significance: 3D printed resins for provisional restorations have become popular with the emergence of new technologies. In this study, we evaluated three different commercially available resins for provisional restorations and one new experimental resin. The results from this study indicate that commercially available resins could be used in clinical settings under certain conditions and limited periods of time. Following the manufacturers protocols is of paramount importance to not compromise these properties.

KEYWORDS

3D print, 3D printed resins, additive manufacturing, finite element analysis, monomers, Weibull

1 | INTRODUCTION

As patents related to additive manufacturing (AM) continue to expire, there is an increasing trend in the accessibility and growth of the 3D printing (3DP) industry.[1] This window of opportunity has led to the development of a range of materials for a multitude of engineering applications, but more importantly for medicine and dentistry.[2,3] Currently, polymeric-based materials account for the vast majority of materials utilized in AM, most commonly referred to as 3DP.[4] One of the first AM methods developed, the stereolithography apparatus (SLA) set the basis for the development of photosensitive resin-based materials, which was achievable using UV laser or UV LED to polymerize specific regions.[4,5]

Digital light projection (DLP) uses high-power LED to two-dimensionally (*x*/*y* axes) polymerize the entire planar area of the build at the same time, contrary to the dynamic laser writing that utilizes SLA technology. While the American Section of the International Association for Testing Materials (ASTM) categorizes DLP into the same category as SLA, Vat-polymerized printing, due to their wide range of similarities, their main difference is the light source,[6] as DLP permits for decreased working times.

The primary advantage of SLA and DLP technologies is their compatibility with various resin systems available on the market. One constant among all commercially available resins is their composition principally in terms of photoinitiators, and UV absorbers that will allow for photopolymerization.[4,7] Many manufacturing techniques have been developed in terms of resin compositions; for example, monomers have the capacity to polymerize in short periods of time, with acrylates and epoxy monomers being the most common.[4] Alternatively, photoinitiators are used in concentrations ranging between 3% and 5% wt; and 3D printers use shorter irradiation exposure, leaving a significant amounts of residual initiator, thus requiring an additional post-curing process, that is, UV curing.[4]

Currently, due to the large variety of 3D printers, post-processing units, and resin systems, there is a wide range of operating procedures with respect to processing and post-processing of materials for dental applications. Among the various post-processing steps, asset of process parameters is modified according to user preferences, such as washing time, UV exposure time, and temperature. Still, most manufacturers do not recommend altering their specific guidelines,[8] which can be a problem for users who acquire 3D printers from different printer manufacturers, while using resins manufactured by yet another company.

Literature reported that some materials with incomplete polymerization can release/diffuse chemical components such as photoinitiators and monomers to the adjacent tissues, affecting them and inducing local and systemic effects, such as cell death via apoptosis and DNA damage.[9–12] The biological risk can be evaluated by performing cell culture and cytotoxicity testing, in vitro.[10] Primary and permanent cell lines may be used to execute a variety of in vitro testing; for example, human fibroblasts derived from periodontal ligament are reproducible when using cells between passages 4–8, and its behavior when in contact with different materials is paramount. Furthermore, it has been established that defective PDL cells may increase the susceptibility to periodontal disease.[13,14]

Mechanical properties of these materials can be affected by a range of factors, which can be associated with (1) the printing technique itself and (2) the materials' composition. Because of the materials' manufacturing process, the printed objects are considered anisotropic.[15] The fact that these materials are polymerized with light, their exposition time and post-curing steps are of vital importance.

In dentistry, the performance of provisional restorations is paramount since they will dictate parameters to be followed and modified according to the patient's needs.[16] Materials commonly used to fabricate these restorations are composite based resins, which have been widely used and available for clinicians for several years; they present some disadvantages associated with their low mechanical properties, such as low-fracture toughness which can lead to critical failure and decreased longevity.[17,18] 3DP technology has been garnered increased popularity among technicians and clinicians due to the wide variety of materials and respective applications, along with ease of use. However, there currently is a lack of evidence with respect to clinical performance, as well as mechanical and biological properties

of 3D materials intended for provisional and/or permanent restorations.

Therefore, due to the paucity of evidence and well-conducted studies regarding mechanical and biological properties of 3D printed polymers for oral restorations the present in vitro study aimed to evaluate the mechanical and biological behavior of different 3D printed polymers for provisional, and potentially, for definitive restorations. The following hypotheses were investigated: (1) there were differences in mechanical properties (biaxial flexural strength and survival probability) among the evaluated resin materials, and (2) there were differences in biological properties (cell viability, proliferation, and cytotoxicity) among different resin materials.

2 | MATERIALS AND METHODS

2.1 | Specimen obtention

Specimens were designed using digital software Shapr3D (Budapest, Hungary) and exported as .stl in high quality. The printing parameters and post-processing steps for each material were strictly followed by the manufacturers who provided the samples. Table 1 presents the composition of each material. Workflow for each material is detailed below:

2.1.1 | Formlabs (FL)

Temporary Crown and Bridge (A3, Formlabs) resin was used to fabricate the specimens, which were loaded into the PreForm software (Formlabs, MA, USA) and the parameters were set to 50-micron layer thickness using the specific exposure time provided by the software for this specific resin. Prints of the specimens were obtained using Formlabs 2 (Formlabs, MA, USA), an automated printer, which automatically set the resin temperature at 35°C. After printing, specimens subjected to the FormWash (Formlabs, MA, USA) for 3 min, an automated washing machine (using 99% isopropyl alcohol [IPA]), used to remove uncured resin from the specimens.

Post-curing was done with FormCure (Formlabs, MA, USA). The curing time was set to 60°C for 20 min as recommended by the manufacturer.

2.1.2 | Crowntec (CT)

The printing process was performed by the manufacturer as follows; AG Saremco print-Crowntec (A3, Saremco, Dental AG, Switzerland) resin was used to fabricate the specimens, which were loaded into Asiga's Composer software (Asiga, Sydney, Australia). Layers of 50-micron thickness were set, as parameters and exposure time was automatically selected depending on the chosen resin.

After printing, cleaning was done by removing excess material with an alcohol-soaked (96%) cloth or brush. All-around cleaning was performed on all specimens until the surface had a matte appearance (specimens are not soaked in alcohol). After cleaning, specimens were air dried with an air syringe. The final curing process was performed with a UV-light box with a wavelength of 320–500 nm, Signum HiLite Power (Kulzer, Hanau, Germany) twice, for 180 s each, turning the specimens between exposure cycles.

2.1.3 | Permanent bridge resin (PB)

Printing process was performed by the manufacturer using PB material (not commercially available, Saremco, Dental AG, Rebstein, Switzerland) resin. The same printing and post-curing process of the CT group were used, according to the manufacturer's guidelines.

2.1.4 | Nextdent (ND)

The printing process was performed by the manufacturer, C&B MFH (N1, Nextdent, 3D Systems, Rock Hill, SC, USA) was shaken by hand for 5 min and then mixed using the LC-3DMixer (Nextdent, 3DSystems, Rock Hill, SC, USA) for 2.5 h. Printing parameters were

TABLE 1 Material composition information given by the manufacturer

Material	Substance name	Concentration (%)
Crowntec (CT)	BisEMA	50 – <70
	Trimethylbenzonyldiphenylphosphine oxide	0.1 – <1
Permanent bridge (PB)	No component disclosure	–
Formlabs (FL)	Esterification products of 4,4′-isopropylidenediphenol, ethoxylated and 2-methylprop-2-enoic acid	> =50 – <75
	diphenyl(2,4,6-trimethylbenzoyl)phosphine oxide	<2.50
Nextdent (ND)	Methacrylic oligomer	>60
	Glycol methacrylate	15–25
	Phosphine oxide	<2.50

set using 3D Sprint software (3DSystems, Rock Hill, SC, USA), 50 microns was set as layer thickness, all other parameters were set automatically by the software upon resin selection. Specimens were printed using Nextdent 5100 (Nextdent, 3Dsystems, Rock Hill, SC, USA). After printing was complete, specimens were cleaned in 91% IPA in an ultrasonic unit for 5 min, carefully dried, and placed into a post-curing unit (LC-3DPrint box, Nextdent, 3D Systems, Rock Hill, SC, USA) for 30 min.

2.2 | Biaxial flexural strength

Disc-shaped specimens ($n = 30$ per group) with 1.2 mm thickness and 14 mm diameter were tested to determine the biaxial flexural strength following ISO 6872:2015 guidelines. The test was performed using a piston-on-three-balls device attached to a universal testing machine (Instron 5566 universal test system, Instron, Norwood, MA, USA) equipped with a ±1000 N load cell. The test was performed at a constant rate of 1 mm/min until failure. The maximum load at failure (*N*), was recorded for each specimen and the following equations were used to calculate biaxial flexural strength (MPa) as per ISO 6872:2015 guidelines:

$$\sigma = \frac{-0.2387\,P\,(X-Y)}{b^2},$$

$$X = (1+v)\ln\left(\frac{r_2}{r_3}\right)^2 + \left(\frac{1-v}{2}\right)\left(\frac{r_2}{r_3}\right)^2,$$

$$Y = (1+v)\left(1+\ln\left[\frac{r_1}{r_3}\right]^2\right) + (1-v)\left(\frac{r_1}{r_3}\right)^2,$$

where, σ = biaxial flexural strength (MPa), P = load at fracture (*N*), b = disc specimen thickness at fracture site, v = Poisson ratio, r_1 = radius of support circle, r_2 = radius of loaded area, and r_3 = radius of the sample. Additionally, Young's modulus was quantified within the linear domain of the stress–strain curve through mechanical testing and quantified using the slope of the line generated within the elastic region (Hooke's Law).

The fractured specimens were examined through Scanning Electron Microscopy (TM400 Plus, Hitachi, Tokyo, Japan) to assess fractographic marks evidence of the fracture origin and direction of propagation. Micrographs of all experimental groups were obtained at 5 kV, with ×40 and ×100 magnifications using SE detector.

2.3 | Finite element analysis

3D finite element analysis (FEA) was conducted, reproducing the same parameters of the biaxial flexural strength testing. SolidWorks 2013 software (Solidworks Corp., Waltham, MA, USA) was used to construct a solid disc (Ø14 × 1.2 mm^2-thick) centrally positioned onto a 3 ball-shaped support. A virtual indenter tip was centrally positioned onto the disc. The model was exported to the Ansys Workbench for numerical simulation.

A 3D mesh was created using tetrahedral-quadratic elements; the maximum size of each element (0.50 mm) was set after a 5% of convergence analysis. The support balls were fully constrained (X, Y, and Z) axis.

The material properties measured at the previous biaxial testing (Young modulus), were used for mechanical characterization. A single FE model is representative of the entire group for most applications. However, considering geometric dimensioning and tolerancing (GDNT) to be one of the limitations of 3DP, it was essential that the FE models be adjusted accordingly. In order to increase accuracy of FEA data, geometry (thickness and diameter) of each of the discs that were utilized for mechanical analysis (biaxial flexural testing) were recorded and were used to generate a custom FE model of that particular disc.

A total of $n = 30$ models per group were created using mechanical properties of the specific materials. The models were considered isotropic, homogeneous, and nonlinearly elastic. A vertical displacement was applied onto the tip toward the disc; loading parameters were set after the pilot test. Data were quantitatively evaluated following the tensile and compression stress and qualitatively evaluated according to the peak-stress distribution. The FEA data was compared to the mechanical testing results.

2.4 | Scanning electron microscopy

High-resolution scanning electron microscopy (SEM) (Hitachi TM400 Scanning Electron Microscopy (Hitachi, Tokyo, Japan) was performed on the specimens ($n = 3$ per group) for surface characterization to assess for topographical information. The SEM micrograph was performed at 15 kV, using SE mode.

2.5 | Assessment of cell viability, proliferation, and cytotoxicity

Thirty disc-shaped specimens (1.2 mm thickness and 6 mm diameter) per group were tested to determine the cell viability and proliferation. After fabrication and sterilization of the materials, the desired number of cells, human periodontal ligament fibroblasts (hPDLF) were seeded (5×10^4/sample) into each well containing one of the materials ($n = 6$/group), plus one control group without material, maintained in an incubator at 37°C with 5% CO_2 levels, and finally assessed for cell viability and proliferation at 24, 48, 72 h, 5 days, and 7 days. Cell viability and proliferation were evaluated using the resazurin-based PrestoBlue assay (#A13262, Invitrogen, CA, USA). Metabolically active cells reduce the PrestoBlue reagent, therefore the colorimetric changes in the media is used to quantify the viability of cells in culture.[19] Fresh media containing PrestoBlue reagent as 1:10 dilution was added to each of the wells and plates were incubated for 30 min. Subsequently, 100 μl of media was removed from each well and

placed into a 96-well plate; absorbance measurements were performed at 570 nm excitation and 600 nm emission wavelengths.

Extracellular lactate dehydrogenase (LDH) in the media can be quantified in which LDH catalyzes the conversion of lactate to pyruvate via Nicotinamide adenine dinucleotide (NAD+) reduction to NADH. Diaphorase then uses NADH to reduce a tetrazolium salt to a red formazan product that can be measured at 490 nm.

The level of formazan formation is directly proportional to the amount of LDH released into the medium. After treatment of cells with extracts, the 50 μl medium was separated from each group into a new 96-well plate. The LDH reaction was performed using a Pierce LDH Cytotoxicity Assay Kit (Thermo Fisher Scientific, NY, USA) following the manufacturer's instructions. The percentage of cytotoxicity was obtained using the following formula:

$$\%\text{cytotoxicity} = \frac{\text{Compound treated LDH activity} - \text{Spontaneous LDH activity}}{\text{Maximum LDH activity} - \text{Spontaneous LDH activity}} \text{x } 100,$$

where the compound treated LDH activity correspond to the cells cultured together with the different materials, the spontaneous LDH activity correspond to cells cultured with ultrapure water, and the maximum LDH activity correspond to cells cultures without any extra compounds.

2.6 | Immunohistochemistry

After 7 days of PrestoBlue analysis, cells were washed with 250 ul of PBS and fixed with 4% paraformaldehyde solution (PFA) overnight at 4°C. After this, three consecutive washes with PBS were performed. Blocking buffer containing 3% BSA, 10% FBS, and 0.2% Triton-X in PBS was added to each sample and kept for 60 min after which was washed with PBS and then incubated with blocking buffer (3% BSA, 10% FBS without Triton-X) containing the primary antibody Phalloidin (Thermo Fisher Scientific, MS, USA) in 1:400 dilution overnight at 4°C. Samples were washed in PBS 3x for 5 min and secondary antibody solution Hoechst 33258 (Thermo Fisher Scientific) in 1:400 dilution was added to the plates, which was covered for 1 h and kept at room temperature. After this time, another wash with PBS was done and samples were kept in PBS.

Images were taken with an Inverted Laboratory Microscope (Leica DM IL LED, Leica, Germany) and channels were merged using ImageJ.

2.7 | Statistical analysis

Data from FEA, cell viability, proliferation and cytotoxicity were tabulated and subjected to descriptive analysis, normality, and homoscedasticity test. Data were statistically evaluated through repeated-measures analysis of variance following post-hoc comparisons by Tukey test, with significance level set at $p < 0.05$. Data are presented as a function of estimated mean values. All analyses were performed using SPSS (IBM SPSS v23, IBM Corp., Armonk, NY).

Biaxial flexural strength data were analyzed using Weibull 2-parameter distribution (Synthesis 9, Weibull ++9, Reliasoft, Tucson, AZ, USA). Weibull modulus (*m*) and characteristic stress (*MPa*) were calculated for all experimental materials and a contour plot was graphed to determine differences between groups (2-sided 95% confidence interval). Additionally, the probability of survival (reliability) as function of characteristic stress was calculated to stresses of 50, 150 and 250 MPa to evaluate their potential clinical performance for provisional restorations.

3 | RESULTS

3.1 | Biaxial flexural strength and probability of survival predictions

Table 2 summarizes the results of the mechanical properties of all tested groups, where Weibull parameters are presented as a function of mean and 95% CI. The calculated Weibull modulus and characteristic stress are depicted in the contour plot presented in Figure 1, where significant differences are detected by the absence of overlap between the contour plots. Regarding characteristic stress, which represents the stress at a failure probability of 62.3%, significantly higher values were observed for PB (249.09 MPa) when compared to CT (208.03 MPa), FL (187.73 MPa), and ND (153.51 MPa), with no differences between CT and FL.

Regarding Weibull modulus (Figure 2), used as a measure to expresses the structural reliability of the material, significantly lower values were observed for FL when compared to CT, PB, and ND, with no statistical differences found between the three groups. Young's modulus was found to be higher for FL (4.671 MPa) when compared to the other materials. CT and PB presented intermediate values (4.04 and 4.001 MPa, respectively) with no significant difference between them, and ND presented the lowest Young's modulus (2.878 MPa) among all tested materials.

The reliability at 50, 150, 250 MPa with the corresponding 95% confidence intervals are presented in Table 3. Analyses of reliability at 50 MPa yielded similar probability of survival for all groups. At 150 MPa, PB presented higher reliability (98%) regarding CT (93%), FL (61%), and ND (43%). Finally, at 250 MPa only PB presented probability of survival above 10% (35%), being significantly superior to the other experimental groups.

All 3D printed polymers presented similar fracture patterns after biaxial flexural strength testing. SEM images evidenced fractographic features such as compression curl (CC), opposite to the surface subjected to tensile stress, and Hackle lines (h), which were used to suggest the origin and direction of the crack propagation (Figure 3).

3.2 | Finite element analysis

Data measurements from FEA are depicted in Table 4. The 3D-printed resin material with the maximum principal (tensile stress) was the ND

TABLE 2 Weibull modulus (m) and characteristic stress (*n*) with their upper and lower 95% confidence bounds for the different materials

	Crowntec (CT)	Permanent bridge (PB)	FormLabs (FL)	NextDent (ND)
Upper bound	217.83	259.75	211.75	161.73
Characteristic stress (MPa)	208.03	249.09	187.73	153.51
Lower bound	198.69	238.87	166.43	145.72
Upper bound	10.87	11.89	4.28	9.64
Weibull modulus (m)	8.2	9.02	3.18	7.23
Lower bound	6.19	6.84	2.37	5.42

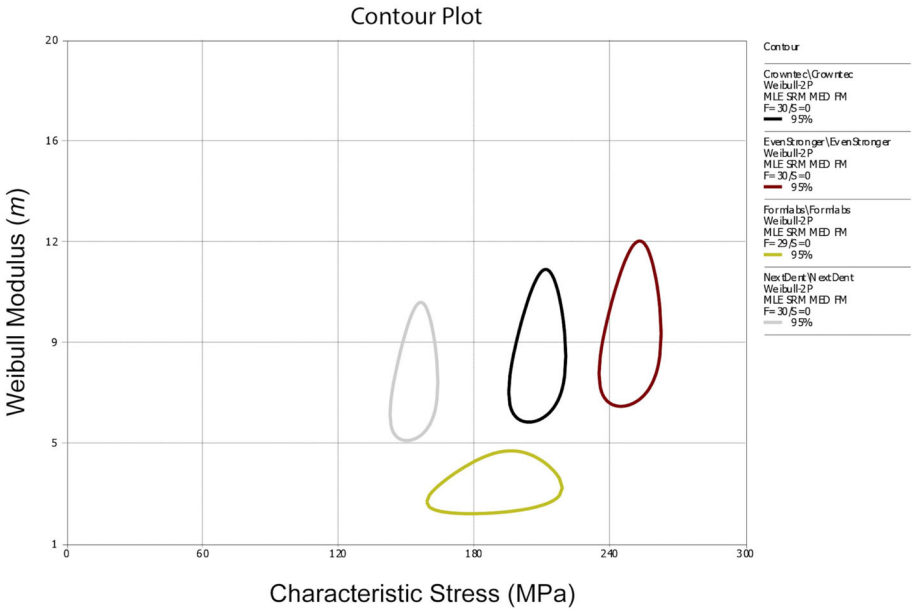

FIGURE 1 Contour plot showing "*m*" as an indicator of reliability (Weibull modulus) versus characteristic stress (*n*), which indicates the stress in which 63.2% of the specimens of each group may fail. The overlap between the groups indicate they are homogeneous

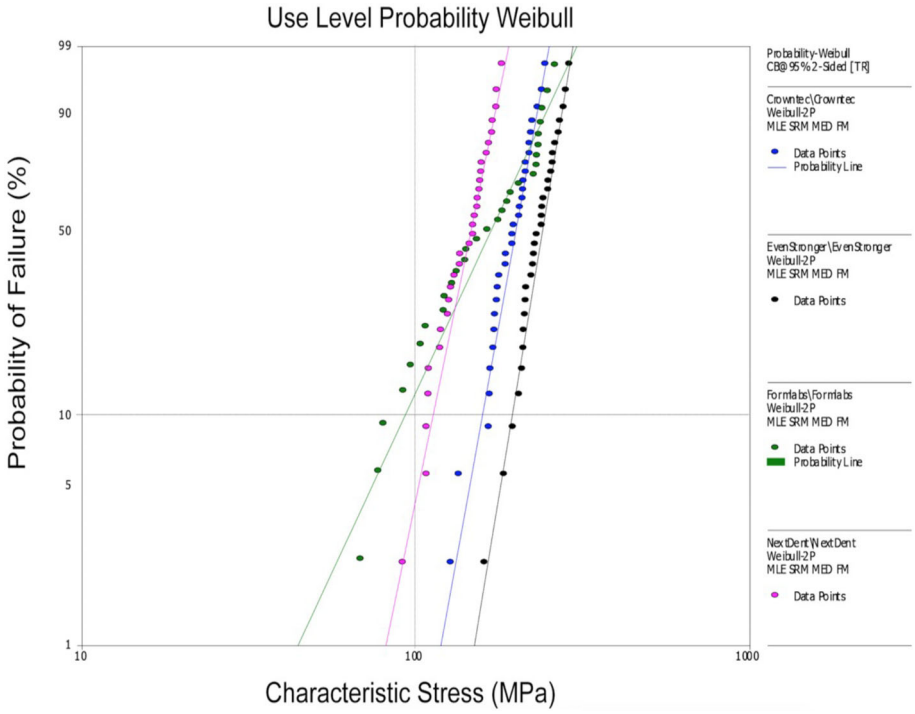

FIGURE 2 Use level probability Weibull, cumulative failure probability plots according to flexural strength (MPa) of 3D-printed resins

TABLE 3 Reliability of different materials under compressive forces as a percentage (%) of the total. Upper and lower bounds are also reported

	50 MPa	150 MPa	250 MPa
Crowntec (CT)	100 (99–100)	93 (84–97)	1 (0–5)
Permanent bridge (PB)	100 (100–100)	98 (95–99)	35 (22–49)
Formlabs (FL)	98 (94–99)	61 (44–74)	8 (2–18)
NextDent (ND)	99 (99–100)	43 (28–56)	0

with 71.65 MPa followed by CT and FL both with 57.37 MPa and last PB with 57.34 MPa. For the minimum principal (compression stress), CT, PB, and FL presented statistically homogenous values, with 103.27 MPa for CT and FL, PB showed values of 103.37 MPa. ND showed values of 93.13 MPa being the lowest one for this parameter. The maximum flexural load was 236.1 MPa for PB material. This value was the greatest of all, with significant differences from all other materials. CT had 196.1 MPa and also had significant differences with all other materials. The third was FL with 167.4 MPa and ND with 143.6, these two had no significant differences in these values.

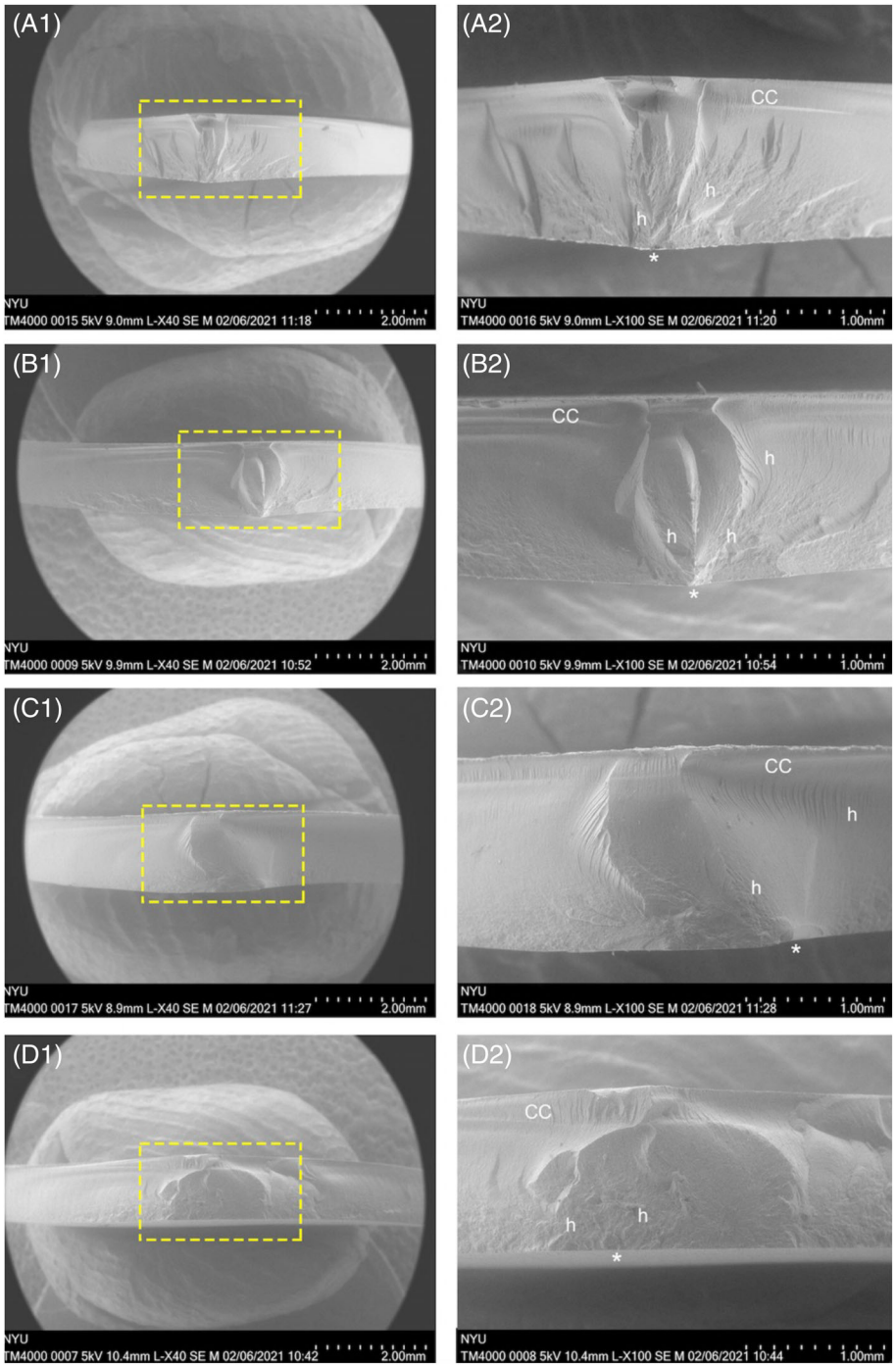

FIGURE 3 Fractography analysis. (A) Crowntec, (B) Permanent bridge, (C) FormLabs, (D) NextDent. CC, compression curve; h, Hackle area. *, suggested fracture origin. All figures with the number 1 were taken at 50x and the figures with number 2 were taken at 150x

TABLE 4 Tensile, compression, shear stress, flexural load, and young's modulus (MPa) of the discs according to the properties of the different materials

	Maximum principal (tensile) (MPa)	Minimum principal (compression) (MPa)	Von-Mises stress (MPa)	Shear stress (MPa)	Maximum flexural load (Mpa)	Young's modulus
Crowntec (CT)	57.37	103.27	68.17	37.76	196.1	4.04
Permanent bridge (PB)	57.34	103.37	68.22	37.82	236.1	4.001
Formlabs (FL)	57.37	103.27	68.17	37.76	167.4	4.671
NextDent (ND)	71.65	93.13	69.57	34.87	143.6	2.878

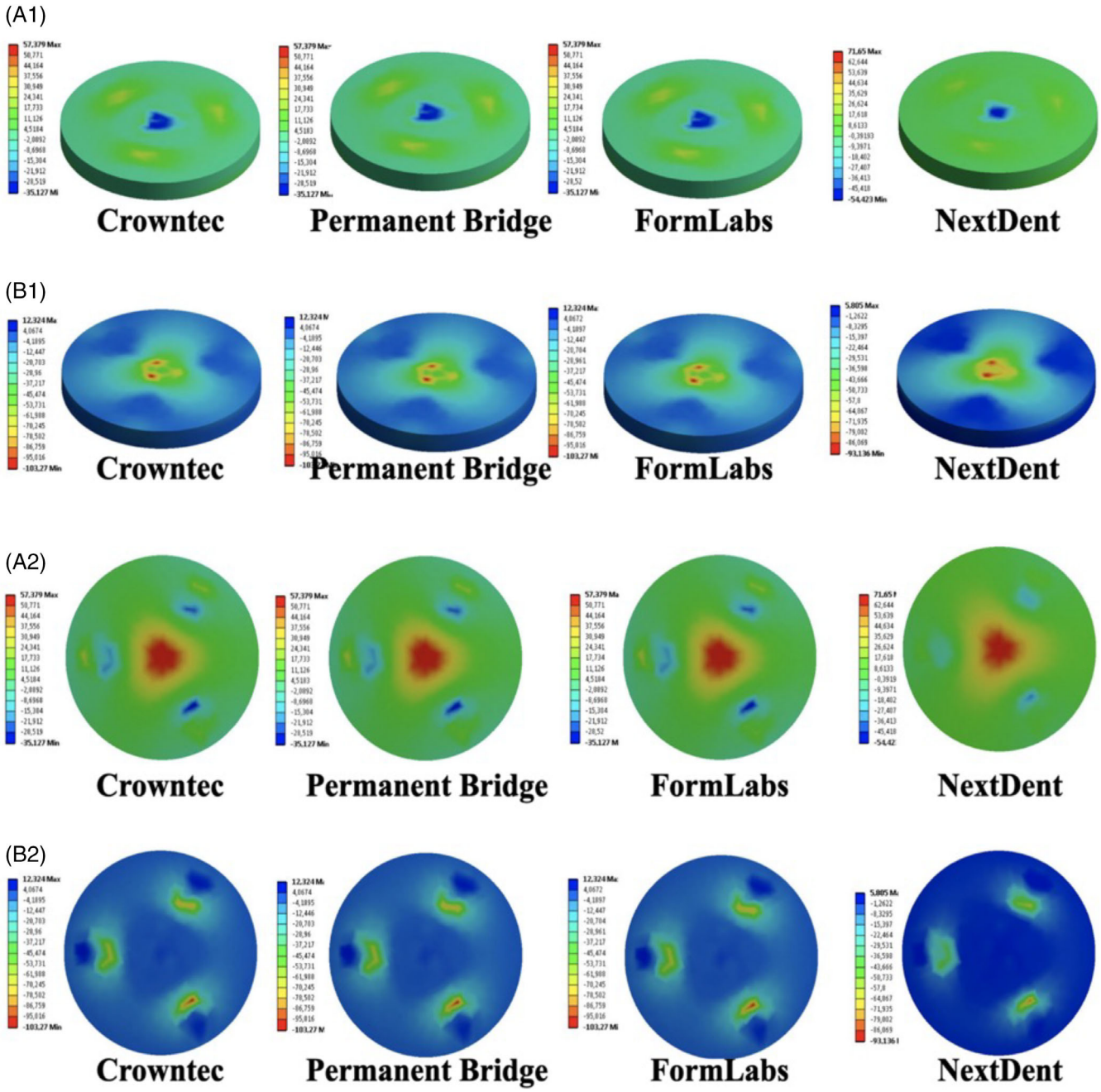

FIGURE 4 (A1–B1): Isometric view of the disc's top surface under tensile (A1) and compression stress (B1). (A2–B2): Isometric view of the disc's bottom surface under tensile (A2) and compression stress (B2)

Isometric view of the disc's top surface under tensile and compression stress is illustrated in Figure 4.

3.3 | Cell viability, proliferation, and cytotoxicity

Images shown in Figures 5 and 6 correspond to cell viability and proliferation with immunohistochemistry. There was no significant difference in cell proliferation of hPDLF cells in contact with different 3D-printed materials. A repeated-measures ANOVA determined that mean proliferation percentage does not differ significantly across the time points ($F = 2.982$ $p = 0.060$). When compared time and groups, there was no significant difference between groups ($p = 0.053$). When evaluating the mean of the materials through all the evaluation time the only one with a significant difference was CT with ND after the Tukey post hoc test ($p = 0.028$).

During the first evaluation time (24 h), ND showed a higher cell proliferation percentage when compared with a control, achieving 86.1%. CT, PB, and FL had 65.3, 64.3, and 63.2 respectively

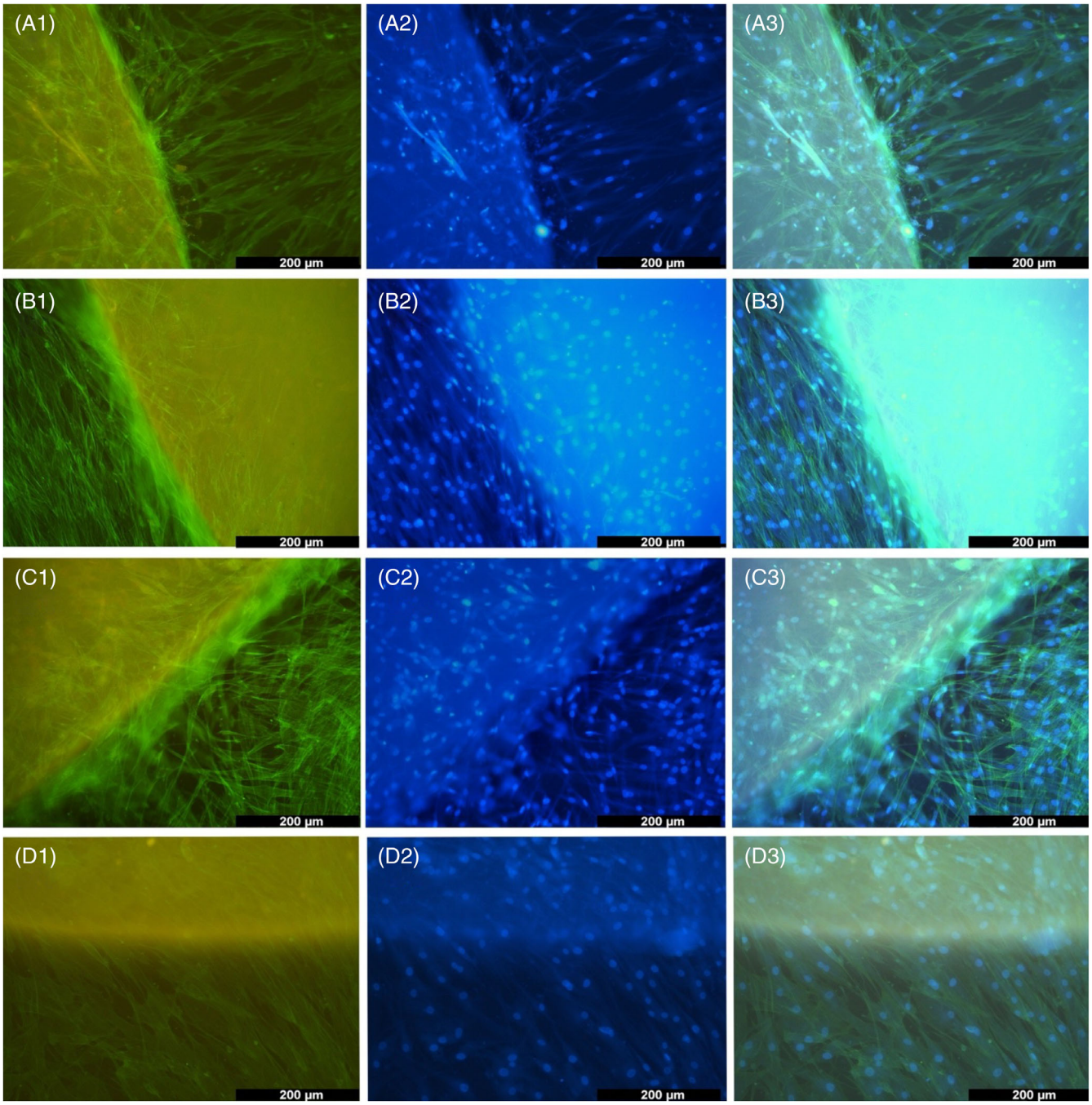

FIGURE 5 Immunohistochemistry were hPDLF cells were stained with Alexa Fluor 488 and Hoechst staining. (A) Crowntec, (B) Permanent Bridge, (C) FormLabs, (D) NextDent. Figures with number 1 represent Alexa Fluor 488 staining, figure with number 2 represent Hoescht staining, and figures with number 3 represent the merged image. hPDLF, human periodontal ligament fibroblasts

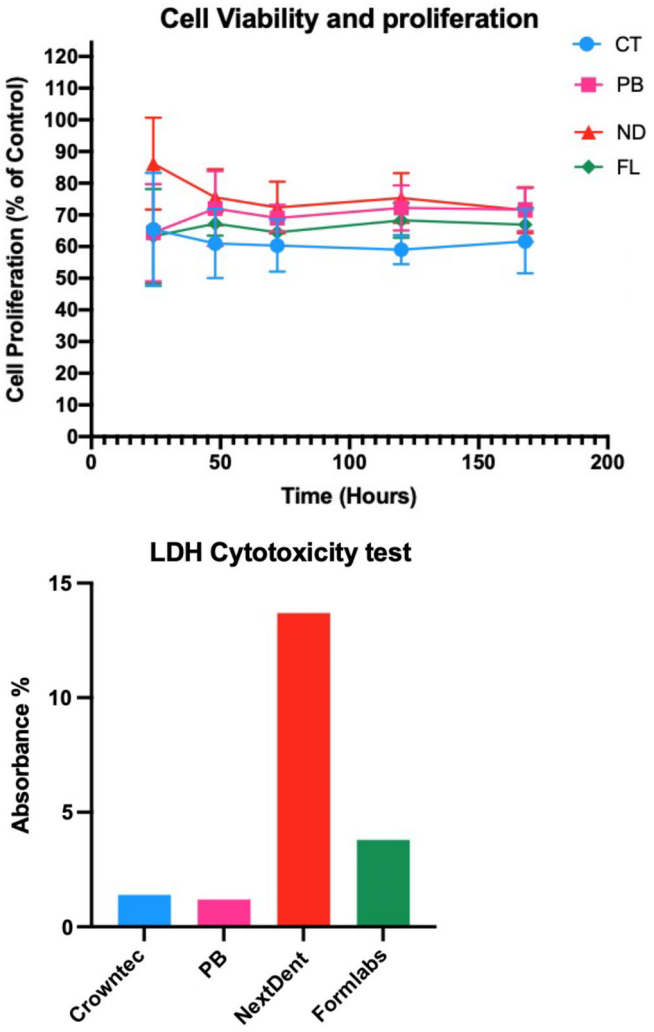

FIGURE 6 Graphic representation of cell viability and proliferation and cytotoxicity with LDH

(Figure 6A). At the terminal evaluation, PB had the best percentage with 71.7%, followed ND with 71.4%. Lastly, we found FL and CT with 66.9% and 61.6% respectively.

Evaluation of cytotoxicity through the LDH assay, yielded no cytotoxicity of the materials (Figure 6B). The highest values for cytotoxicity were recorded for the ND followed by FL at 13.7% and 3.8%, respectively. Both CT and PB showed cytotoxicity values below 2% (1.4% and 1.2% respectively).

4 | DISCUSSION

3D printed resins have gained popularity among clinicians due to some advantages such as reduce of designing times, expedite fabrication, and improved performance. Similar to what happens to resin composites, there are a variety of factors that can influence the final materials properties such as particle size, shape, monomer type, flowability, and viscosity, also, some inherent characteristics of these types of materials and equipment used for its polymerization such as the polymerization time, light source used, and its post processing steps.

Numerous clinical techniques have been published elsewhere, however due to the increased popularity and variety of new materials intended for oral applications, the lack of scientific literature related to the materials inherent properties and appropriate workflows raises a concern about the survival and the expected mechanical complications. The results from this report provide an insight onto the mechanical and biological properties of different 3D printed materials intended for provisional restorations following the manufacturers acquisition protocol.

Fractographic analysis of the samples submitted to the single load to failure test confirmed the absence of critical defects in the corner area of the fracture surface. This finding along with fractographic features suggests that the maximum tensile stresses were concentrated at the central area of the discs, where the failure initiated. Such concentration of stress allows an accurate measurement of the load necessary to fracture the specimens and has been considered a reliable method to assess the mechanical properties of restorative materials. Furthermore, the analyses of the data through Weibull statistics allowed for the calculation of the Weibull modulus, that represents the structural reliability of the

material, and the characteristic stress, that indicates the stress at which 63.2% of the specimens would fail. Among all the materials tested in the present study, PB presented the higher mechanical performance. This was observed not only in terms of characteristic stress, but also in the probability of survival analyzed at 150 and 250 MPa, where PB presented higher reliability when compared to the other groups.

At the lower stress (50 MPa), which is considered a minimum flexural strength requirement for polymer-based crowns, all the materials tested demonstrated high reliability. However, it is noteworthy to mention that the minimum requirement of 50 MPa established at the ISO 10477 was based on flexural strength test on a three-point bending fixture. While a lack of consensus has been observed in the mechanical evaluation of resin composite materials in dentistry, it has also been suggested that biaxial flexure testing methods provide more reliable results than three-point flexure. Nevertheless, considering the differences in three-point bending and biaxial flexural strength tests, comparisons among studies should be made with caution.

The FEA showed that, tensile stress peak was located at the opposite surface of the loading tip (compression peak) regardless of material property which corroborates with fractography findings. One parameter that has been shown to affect the mechanical properties of 3D printed materials is the printing orientation which also affects printing accuracy, surface characteristics, among others, meaning that polymerization of the monomers also varies with the object orientation, due to the fact that light must penetrate a specific depth into the monomer, and that adhesion between successive layers is weaker than the strength within the same layer.[1]

When evaluating the biological properties, among different materials, ND and PB yielded the most favorable results in terms of cell viability and proliferation. Different materials were subjected to different printing and post-processing protocols, following the manufacturer's guidelines. This is important, as different resins made for 3DP have specific components, such as monomer composition, photoinitiators and pigments.

In terms of cell proliferation, there was a higher proliferation of hPDLF cells in the ND material after 24 h, which decreased after 48 h. This change in proliferation explains the higher degrees of LDH present. It should be noted that the present study did not evaluate LDH for longer time points, although it is expected to observe a decrease in this value and a tendency to achieve similar results to the other materials in line to what we observed in the proliferation analysis.

There is evidence supporting the correlation between degree of conversion, mechanical performance, and biological effects of different dental resin composites,[9] which suggests that residual monomers have the capacity to induce cytotoxicity and cause genotoxic effects.[20] The present results did not indicate cytotoxic effects (LDH assay) nor affected cell proliferation significantly, which highlight the importance of following the manufacturer's guidelines when acquiring materials intended for intraoral use, diminishing possible side effects due to, for example, incomplete resin polymerization and presence of residual monomers. It is unclear which parameters each manufacturer uses for their specific resins since the profiles are preloaded in their software. Further studies comparing alternative printing protocols should be carried out to validate different printers and resin polymerization parameters.

In the present study, CT and PB groups achieved Characteristic Stress results similar to some CAD/CAM, bulk/fill, and conventional resin materials, which might indicate its potential use as long-term restorative materials. However, further in vitro studies evaluating the mechanical performance of these materials in anatomical samples submitted to cyclic loading, as well as controlled clinical trials are warranted.

It is important to note that manufacturers do not provide the specific chemical composition of their resin, that is, the organic composition, or inorganic fillers (wt%). The only information provided is the use of monomer-based acrylic esters with Class IIa CE certification, which allows the installation of this material in the body for up to 30 days.[6] The absence or the use of different filler particles and amounts, can affect the final properties. This might restrain the use of their material in 3D printers other than theirs.

Another aspect that this current article did not evaluate is the fact that different polishing protocols may have a significant effect on the mechanical and biological properties of these materials. It has been reported in the literature, especially regarding zirconia, that different type of cellular unions can be formed depending on this aspect.

Therefore, factors such as resins' composition (monomers, fillers, pigments, among others), light intensity/exposure, and printing orientation affect the mechanical and biological properties of 3D printed resins. It is of paramount importance, for both research and evidence-based dentistry, to follow the manufacturers' guidelines when indicating these materials to avoid misinterpretation of its inherent properties.

5 | CONCLUSION

Within the limitations of this study, it was concluded that: (1) There were differences in BFS and Probability of survival prediction among the different evaluated resin materials intended for 3DP use, and (2) There were no differences in cell viability, cell proliferation, and cell toxicity among different evaluated resin materials.

ACKNOWLEDGEMENT AND DISCLOSURE

The authors would like to thank Saremco and Nextdent for providing the materials used in this study. The authors declare no conflict of interest.

DATA AVAILABILITY STATEMENT

The data that support the findings of this study are available from the corresponding author upon reasonable request.

ORCID

Pablo J. Atria https://orcid.org/0000-0001-6298-9756
Dimorvan Bordin https://orcid.org/0000-0002-8466-9558
Julian Conejo https://orcid.org/0000-0002-2318-0580
Lukasz Witek https://orcid.org/0000-0003-1458-6527
Camila S. Sampaio https://orcid.org/0000-0002-2517-7684

REFERENCES

1. Tahayeri A, Morgan MC, Fugolin AP, et al. 3D printed versus conventionally cured provisional crown and bridge dental materials. *Dent Mater*. 2018;34:192-200.
2. Best C, Strouse R, Hor K, et al. Toward a patient-specific tissue engineered vascular graft. *J Tissue Eng*. 2018;9:2041731418764709.
3. Shubert J, Bell MAL. Photoacoustic imaging of a human vertebra: implications for guiding spinal fusion surgeries. *Phys Med Biol*. 2018; 63:144001.
4. Stansbury JW, Idacavage MJ. 3D printing with polymers: challenges among expanding options and opportunities. *Dent Mater*. 2016;32: 54-64.
5. Kaplan H. Stereolithography-a marriage of technologies. *Photonics Spectra*. 1990;24:74.
6. Revilla-León M, Meyers MJ, Zandinejad A, Özcan M. A review on chemical composition, mechanical properties, and manufacturing work flow of additively manufactured current polymers for interim dental restorations. *J Esthet Restor Dent*. 2019;31:51-57.
7. Khorsandi D, Fahimipour A, Abasian P, et al. 3D and 4D printing in dentistry and maxillofacial surgery: printing techniques, materials, and applications. *Acta Biomater*. 2021;122:26-49.
8. Kessler A, Hickel R, Reymus M. 3D printing in dentistry—state of the art. *Oper Dent*. 2020;45:30-40.
9. Manojlovic D, Dramićanin MD, Miletic V, Mitić-Ćulafić D, Jovanović B, Nikolić B. Cytotoxicity and genotoxicity of a low-shrinkage monomer and monoacylphosphine oxide photoinitiator: comparative analyses of individual toxicity and combination effects in mixtures. *Dent Mater*. 2017;33:454-466.
10. Geurtsen W, Lehmann F, Spahl W, Leyhausen G. Cytotoxicity of 35 dental resin composite monomers/additives in permanent 3T3 and three human primary fibroblast cultures. *J Biomed Mater Res: Off J Soc Biomater Japanese Soc Biomater Australian Soc Biomater*. 1998; 41:474-480.
11. Ferracane J. Elution of leachable components from composites. *J Oral Rehabil*. 1994;21:441-452.
12. Michalakis K, Pissiotis A, Hirayama H, Kang K, Kafantaris N. Comparison of temperature increase in the pulp chamber during the polymerization of materials used for the direct fabrication of provisional restorations. *J Prosthet Dent*. 2006;96:418-423.
13. Lehmann F. Usefulness of primary gingival fibroblast cultures for cytotoxicity tests. *J Dent Res*. 1996;175:1896.
14. Barczyk M, Olsen L-HB, da Franca P, et al. A role for α11β1 integrin in the human periodontal ligament. *J Dent Res*. 2009;88:621-626.
15. Reymus M, Fabritius R, Keßler A, Hickel R, Edelhoff D, Stawarczyk B. Fracture load of 3D-printed fixed dental prostheses compared with milled and conventionally fabricated ones: the impact of resin material, build direction, post-curing, and artificial aging—an in vitro study. *Clin Oral Investig*. 2020;24:701-710.
16. Balkenhol M, Mautner MC, Ferger P, Wöstmann B. Mechanical properties of provisional crown and bridge materials: chemical-curing versus dual-curing systems. *J Dent*. 2008;36:15-20.
17. Aati S, Akram Z, Ngo H, Fawzy AS. Development of 3D printed resin reinforced with modified ZrO2 nanoparticles for long-term provisional dental restorations. *Dent Mater*. 2021;37:e360-e374.
18. Benalcazar Jalkh E, Machado CM, Gianinni M, et al. Effect of thermocycling on biaxial flexural strength of CAD/CAM, bulk fill, and conventional resin composite materials. *Oper Dent*. 2019;44:E254-E262.
19. Tynan RJ, Weidenhofer J, Hinwood M, Cairns MJ, Day TA, Walker FR. A comparative examination of the anti-inflammatory effects of SSRI and SNRI antidepressants on LPS stimulated microglia. *Brain Behav Immun*. 2012;26:469-479.

How to cite this article: Atria PJ, Bordin D, Marti F, et al. 3D-printed resins for provisional dental restorations: Comparison of mechanical and biological properties. *J Esthet Restor Dent*. 2022;1-12. doi:10.1111/jerd.12888